

Fault Diagnosis in Semiconductor Etch Equipment Using Bayesian Networks

Javeria Muhammad Nawaz, Muhammad Zeeshan Arshad, and Sang Jeen Hong*

Abstract—A Bayesian network (BN) based fault diagnosis framework for semiconductor etching equipment is presented. Suggested framework contains data preprocessing, data synchronization, time series modeling, and BN inference, and the established BNs show the cause and effect relationship in the equipment module level. Statistically significant state variable identification (SVID) data of etch equipment are preselected using principal component analysis (PCA) and derivative dynamic time warping (DDTW) is employed for data synchronization. Elman's recurrent neural networks (ERNNs) for individual SVID parameters are constructed, and the predicted errors of ERNNs are then used for assigning prior conditional probability in BN inference of the fault diagnosis. For the demonstration of the proposed methodology, 300 mm etch equipment model is reconstructed in subsystem levels, and several fault diagnosis scenarios are considered. BNs for the equipment fault diagnosis consists of three layers of nodes, such as root cause (RC), module (M), and data parameter (DP), and the constructed BN illustrates how the observed fault is related with possible root causes. Four out of five different types of fault scenarios are successfully diagnosed with the proposed inference methodology.

Index Terms—Fault diagnosis, bayesian inference, fault detection and classification

I. INTRODUCTION

Semiconductor manufacturing processes became more complex over the decades due to the continuous needs for smaller and higher density chips. The advancement in semiconductor manufacturing technology increases the demand of higher level of manufacturing process control with improved precision for satisfying narrower process margins in manufacturing. In process control, statistical process control (SPC) is widely used for finding the source of variation in a given process to maintain consistent product quality, but it holds the lack of timeliness due to the post process metrology. When a fault is detected, the process is halted, and a corrective action needs to be promptly taken with identifying the actual source of variation in the equipment. Correct diagnosis can contribute to reducing equipment downtime as compared to the traditional 'hit and trial' approach to identify the source of fault. Any delay in process control in high volume manufacturing may cause extended machine down time, which would affect the production yield as well as manufacturing throughput. Therefore, the detection of an incipient fault run as well as its classification is critical to improve the production yield in high volume semiconductor manufacturing.

Semiconductor manufacturing equipment consists of a few hundred built-in sensors for monitoring the tool status and the process. Sensory data contains full of useful information of the equipment status and the corresponding process, and it can be utilized for the detection of an incipient fault on wafer-in-process; however, the handling of large amount of equipment data is arduous. In our previous research, we demonstrated the usefulness of artificial intelligence algorithm with

evidential reasoning as a promising candidate for a method of equipment fault detection and classification (FDC) [1]. Goodlin et al. have used fault-specific control charts to detect and classify faults in an etcher using FDC data [2]. Ison et al. have presented a tree based modeling technique to classify faults [3]. Barrios et al. have presented an auto-associative neural network based approach for diagnosing faults [4]. Similarly, Baluja et al. have proposed five artificial neural networks based techniques for the purpose [5]. However, limited physical understanding of the process equipment and the complex operational relationship in sub-system level associated with the process is considered in previous research.

In this research, we propose a Bayesian network (BN) based inference methodology for fault diagnosis of semiconductor manufacturing equipment. Diagnostic inference was performed based on a cause and effect analysis with physical understanding of 300 mm wafer manufacturing equipment. In data preprocessing phase, the statistically significant state variable identifier (SVID) were selected through principal component analysis (PCA) and synchronized using the derivative dynamic time warping (DDTW) algorithm. Elman’s recurrent neural network (ERNN) was employed for the prediction of time series data and the assignment of conditional probabilities in BNs, and eventually fault diagnosis was demonstrated by the combination of fault conditional probabilities including expert knowledge and process information of the semiconductor manufacturing equipment. The rest of the paper is divided into four sections.

Section II provides a theoretical background of BN inference. The proposed diagnostic methodology for RIE etcher is discussed in Section III. Section IV presents the implementation and fault diagnostics of the proposed technique using 300 mm etch equipment model which is reconstructed in subsystem levels. Finally, results and conclusion are provided in Section V.

II. THEORETICAL BACKGROUND

1. Bayesian Network

A Bayesian network (BN) is one of the preferred methods for the inference of cause and effect relationship. BN, also known as probability or belief networks, is used

for the representation of dependencies within a set of random variables in the form of a directed acyclic graphs where the nodes represent the random variables and the arrows represent the causal relationship between them [6]. The arrow leads from a node representing the cause variable to the node representing the effect variable. For all root nodes which have no parents, only unconditional prior probabilities are defined, while for all other nodes, the conditional probability distribution (CPD) in the form of a table is defined with respect to the occurrence of their parent nodes.

Taking an example out of the semiconductor equipment, Fig. 1 shows a BN of a fault in gas delivery system. If a mass flow controller (MFC) is not calibrated correctly (represented by node A), it would allow more or less gas to flow into the chamber, which would be detected as fault in gas flow (represented by node B). The incorrect amount of gas flow will then affect the flow sensor reading of the total gas flow in the gas splitter, and this can result in a fault in its observation (represented by node C).

Here the prior probability for root node A is defined as the unconditional probability $P(A)$, while CPDs for nodes B and C are defined as conditional probabilities with respect to the occurrence of their parents, $P(B|A)$ and $P(C|B)$ respectively. These values are obtained from process knowledge and expert opinion. For any Bayesian network for a set of random variables $\{X_1, X_2, X_3, \dots, X_i\}$, the joint probability of all variables in the network can be expressed as the product of the CPD of each node given its parents. Mathematically,

$$P(X) = \prod_{i=1}^n P(X_i | \text{parents of } (X_i))$$

One of the several advantages of the BN is, once the relationships between the variables are defined through the network structure and probabilities, inference can be

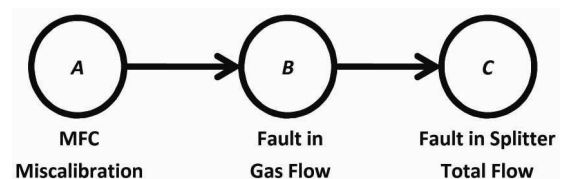


Fig. 1. Example Bayesian Network for fault in gas.

performed. Inference is the procedure of finding the posterior probability of a specific variable in the network when exact values of other variables are provided. These known values of variables are called the evidences. The effect of the evidences propagates through the network, and incorporating this new information the BN computes the revised probability of each node in the network. This is equivalent to saying that the BN combines the newly found evidences from the prior information to obtain an improved judgment for the status of each variable. For a diagnostic problem, the evidences are actually the symptoms observed in the system, and to diagnose or inference the root cause of the problem, BNs rely on the Bayes' theorem which is mathematically defined as

$$P(A|B) = \frac{P(B|A)P(A)}{P(B)}$$

2. Inference Example

In order to demonstrate how a BN can be used for fault diagnosis, let's consider a simple example as presented in Fig. 1. Suppose the prior probability for node A , $P(A=True)=0.3$ i.e. the probability of MFC mis-calibration is 0.3. For the nodes B and C , CPDs are represented in the form of conditional probability tables as shown in Table 1.

At this point, we can calculate the marginal probability for each node which is the simple probability of that node, can be found using the formula for marginal probability

$$P(A) = \sum_B P(A|B) \times P(B).$$

Using this equation we get $P(A)=0.3$, $P(B)=0.31$ and $P(C)=0.317$. Now let's suppose that the evidence was found that the total flow of gas in splitter is not normal. This implies that we have ($C=True$). Now using this new evidence the posterior probability of node B and C can be found making use of the Bayes' theorem as

$$P(B|C) = \frac{P(C|B)P(B)}{P(C)} = \frac{0.8 \times 0.31}{0.317} = 0.775$$

$$\begin{aligned} P(A|C) &= \frac{P(C|A)P(A)}{P(C)} \\ &= \frac{[P(C|A,B)P(B|A) + P(C|A,\sim B)P(\sim B)] \times P(A)}{P(C)} \\ &= \frac{0.66 \times 0.3}{0.317} = 0.624 \end{aligned}$$

$$\begin{aligned} P(A|C) &= \frac{P(C|A)P(A)}{P(C)} \\ &= \frac{[P(C|A,B)P(B|A) + P(C|A,\sim B)P(\sim B)] \times P(A)}{P(C)} \\ &= \frac{0.66 \times 0.3}{0.317} = 0.624 \end{aligned}$$

$$\begin{aligned} P(A|C) &= \frac{P(C|A)P(A)}{P(C)} \\ &= \frac{[P(C|A,B)P(B|A) + P(C|A,\sim B)P(\sim B)] \times P(A)}{P(C)} \\ &= \frac{0.66 \times 0.3}{0.317} = 0.624 \end{aligned}$$

We infer that MFC has been out of calibration with a probability of 0.624. This example shows how Bayesian networks can be very useful to model and diagnose a fault diagnosis problem, and in this manner, we can have diagnostic inference for fault diagnosis with evidence combination.

III. DIAGNOSTIC METHODOLOGY

1. System Apparatus

We employed a capacitive coupled plasma-reactive ion etching (CCP-RIE) system for diagnostic inference study. RIE is one of the most important processes in semiconductor device manufacturing, where reactive ions are used to selectively remove layers of solid films on the a wafer [7]. A simplified schematic of the RIE etcher is shown in Fig. 2. The wafer is placed on an electrostatic chuck (E-Chuck) in vacuum chamber, where process gases are provided inside the chamber. Two parallel plates at the top and bottom of the chamber in capacitive coupled plasma (CCP) system act as electrodes and are connected to an RF generator which is used to excite the gas to generate plasma. The smaller size of the powered electrode as compared to the grounded electrode causes a negative DC bias at the powered electrode, which results in high energy positive

Table 1. CPT'S defined for the nodes B and C

A	P(B=True)	P(B=False)	B	P(C=True)	P(C=False)
True	0.80	0.10	True	0.80	0.10
False	0.20	0.90	False	0.20	0.90

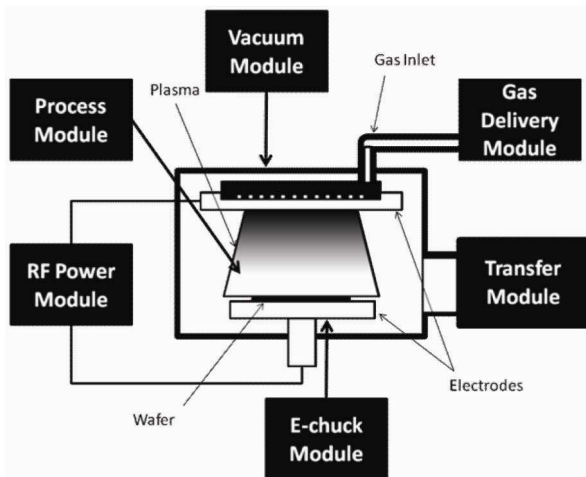


Fig. 2. Schematic of RIE Etcher System divided into modules.

ion bombardment on the wafer placed at the electrode. This bombardment etches the target layer on the wafer.

Occurrence of any fault in RIE etcher may damage the wafers being processed. In case of such a fault in the process or equipment, it must be detected to avoid scraping of more wafers and avoid further misprocessing, but another important issue is that the equipment must be properly diagnosed to eliminate cause of the fault. A diagnostic system that could detect faults and properly classify them is critical to enhance the manufacturing effectiveness. When a fault occurs in RIE in reality, the effects of a fault can be observed in more than one part of the system, and this makes it difficult to just point out the exact root cause. In order to simplify the system we have divided the system into six modules as shown in Fig. 2, such as RF power module, gas delivery module, process chamber module, vacuum module, E-chuck module and transfer module. The RF power module consists of all power related components in the etcher, and the key components are RF generator and the matcher. All components of the system related to delivery of gases, for example the MFCs and flow splitters, into the chamber are included in the gas delivery module. Similarly, the process chamber module includes the components dealing with the process. Vacuum module contains components that are related to vacuum generation and control. Likewise, components in the system that are associated with the E-chuck are included in the E-chuck module. Components that deal with the transfer of wafers to and from the process chambers are included in the transfer module. This

categorization makes it easier to analyze the cause and effect of the system in one level down at the sub-system (or module) level.

2. Cause and Effect Analysis

In order to design a fault diagnosis system, as many faults that could occur in the system must be taken into consideration as possible in order avoid misleading result. Hence we construct a fishbone diagram which is a good way to carefully analyze, determine and list up all the potential causes of a problem or their effects in visual representation. It also makes way for generating better model for the diagnosis of faults. The fishbone diagram constructed for faults in RIE is shown in Fig. 3. The main bone represents the faults in semiconductor etch equipment. The branches represent sub-system level modules. The smaller bones branching from the sub-bones represent the causes of faults within each module. The construction of fish-bone diagram involved brainstorming by incorporating equipment, process and expert knowledge.

3. Construction of Bayesian Network

In order to make use of a Bayesian network for a given problem, the first step is defining the network structure. Structure of a Bayesian network can be learned from data for some problems, but it generally relies on process, equipment and expert knowledge for diagnosing a fault in semiconductor equipment. We propose a three layer Bayesian network for the diagnosis of faults using SVID data as shown in Fig. 4. The top layer corresponds to the root causes, the middle layer corresponds to faults observed in modules, and the bottom layer corresponds to faults observed in SVID data parameters. The evidence would be added to the bottom layer, which can be inferred to find the most probable root cause from the top layer.

Following this framework, we defined a structure of cause and effect diagram in the semiconductor etcher in Fig. 5 for which the node descriptions are provided in Table 2. Each module has been assigned as a node, representing the fault observed in that module and is connected to its child node of all the root nodes for the respective modules. Next the child nodes of each module

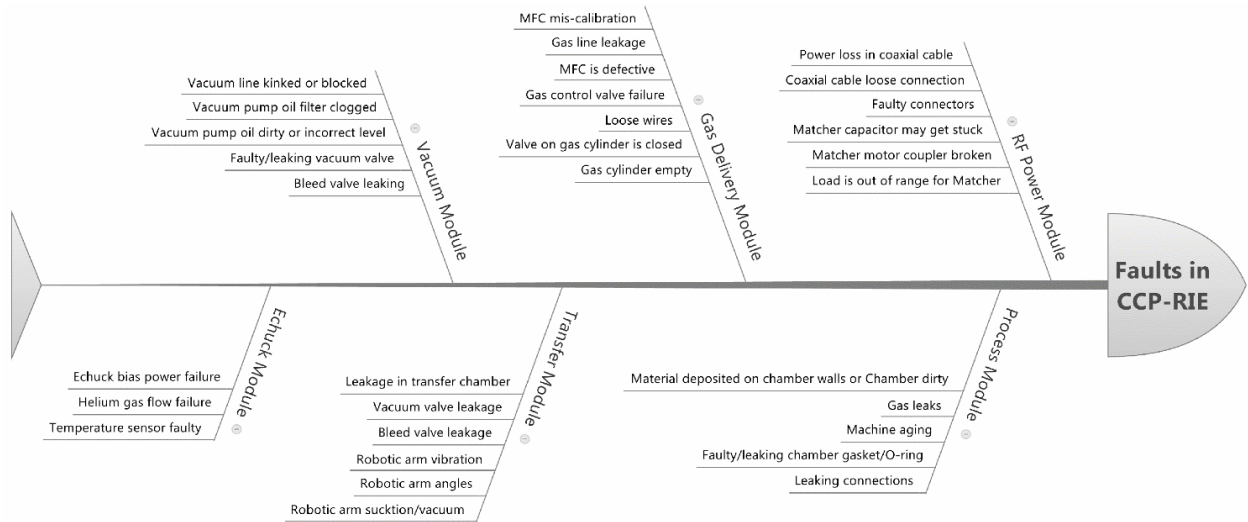


Fig. 3. Fishbone diagram for faults in CCP-RIE.

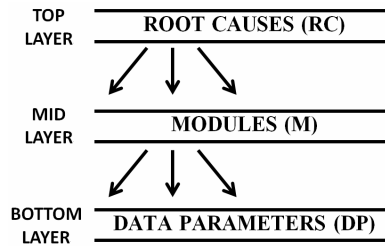


Fig. 4. Proposed three layer design of Bayesian network.

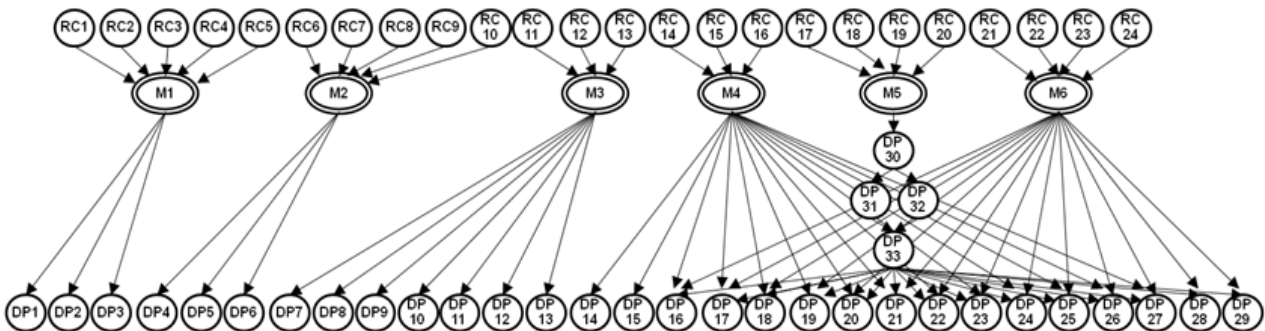


Fig. 5 Bayesian network for the fault diagnosis in RIE etch equipment.

node represent the fault observed in SVID data as a result of direct or indirect effect of fault occurrence within that module. We tried to model the relationships between different causes and their effects. The network shows direct and indirect effects of faults that could appear in different modules, but it ends up being observed on some common set of parameters. This shows the complexity of the intertwined components of the system that make it difficult to model and diagnose. The given BN is a general network that could be applied to any kind of etch

system with little or no changes because the faults and relationships are more or less the same in all kinds of plasma etch systems. This can be considered as generalized framework which can be extended to diagnose any fault in other kinds of semiconductor equipment as well. For example, being very similar to plasma etch equipment, the plasma enhanced chemical vapor deposition (PECVD) systems can also employ this framework for diagnosis of faults.

Table 2. Nodes Description for the Network of Fig. 5

Node	Description	Node	Description
RC1	Bleed valve leaking	DP3	Vacuum valve position
RC2	Vacuum valve	DP4	Robot arm position
RC3	Vacuum sensor	DP5	Robot arm angles
RC4	Poor vacuum conduction	DP6	Transfer module pressure
RC5	Throttle valve	DP7	Helium pressure
RC6	Leakage in transfer chamber	DP8	Helium leak rate
RC7	TR chamber V. valve leak	DP9	Helium pressure set point
RC8	TR chamber V. valve leak	DP10	Helium flow rate
RC9	Robotic arm vibration	DP11	E-chuck voltage reading
RC10	Robotic arm angles	DP12	E-chuck current reading
RC11	E-chuck bias power failure	DP13	Wafer temperature
RC12	Helium gas flow failure	DP14	Source forward reading
RC13	Faulty temperature sensor	DP15	Bias forward reading
RC14	Power loss in coaxial cable	DP16	Source reflected reading
RC15	RF Cable loose connection	DP17	Bias reflected reading
RC16	Matcher fault	DP18	RF Matcher: Cap. reading
RC17	MFC miscalibration	DP19	RF Matcher: Current 1
RC18	Gas line leakage	DP20	RF Matcher: Current 2
RC19	Gas cylinder empty	DP21	RF Matcher: Series
RC20	Gas control valve failure	DP22	RF Matcher: Shunt
RC21	Chamber wall deposition	DP23	RF probe: voltage
RC22	Particles	DP24	RF probe: current
RC23	Chamber leak	DP25	RF probe: phase
RC24	Gasket/O-ring wear out	DP26	RF probe: V_{pp}
M1	Vacuum Module	DP27	RF probe: DC bias
M2	Transfer Module	DP28	TGV Valve position
M3	E-chuck Module	DP29	Pressure
M4	RF Module	DP30	Gas flow rate
M5	Gas Delivery Module	DP31	Flow splitter: Flow 1
M6	Process Chamber Module	DP32	Flow splitter: Flow 2
DP1	Bleed valve position	DP33	Flow splitter: Total flow
DP2	Throttle valve position		

IV. IMPLEMENTATION

1. Data Acquisition and Preprocessing

Data used for the purpose of this research was SVID data, acquired from Applied Materials’ DPS-II Centura dielectric etcher. It consisted of 10 healthy runs and intentionally induced 5 faulty runs with different types of faults. The faulty runs are suggested by equipment engineers based on their most frequent experience, and they are presented in Table 3. Our purpose is to diagnose these faults to demonstrate and assess the functionality of the proposed technique. The data was composed of 55 parameters corresponding to different modules of the equipment. This data is used for the construction of BN

Table 3. Faults added in different runs

Run ID	Fault Induced
Exp.1	-1% MFC conversion shift
Exp.2	+1% MFC conversion shift
Exp.3	Source RF Cable: loss simulation
Exp.4	Bias RF Cable: power delivered
Exp.5	Added chamber leak by 1.3 mT/min

Table 4. List of parameters selected through PCA for fault detection

Par.	Par. Name	Par.	Par. Name
1	Throttle Gate Valve Current	9	RF Probe Phase
2	RF Source Forward	10	E-chuck Voltage
3	RF Matcher Current 1	11	Flow Splitter-Flow 1
4	RF Matcher Current 2	12	Flow Splitter-Total Flow
5	RF Bias Forward	13	Gas Flow-12
6	RF Bias Shunt	14	RF Probe V_{pp}
7	RF Probe Voltage	15	RF Probe DC Bias
8	RF Probe Current		

and the evidence generation for inference of faults. The original data consisted of 55 parameters collected at a frequency of 10 Hz. For an efficient use of SVID data in a fault diagnosis system, the data must be reduced by selecting only those parameters that carry useful information. For this purpose, we made use of principle component analysis (PCA) which can be used to select statistically most significant parameters [8].

Out of the 55 parameters, 15 parameters represented in Table 4, were selected by PCA. As each parameter in the SVID data has its own range of values; therefore, it is appropriate to normalize the data to a fixed range [0, 1] before subsequent steps. Apart from normalization another issue is that SVID data collected for various runs is not synchronized i.e. the number of observations for each run varies due to slight differences in duration of each run. This problem must be addressed before the data can be used. Hence, derivative dynamic time warping (DDTW) algorithm was employed to synchronize the data [9].

2. Bayesian Inference

For the Bayesian inference of this diagnostic problem, using the general network in Fig. 5, we define a BN structure dedicated for this problem as shown in Fig. 6. The node description for the network is provided in Table 5. BN structure design and the subsequent steps

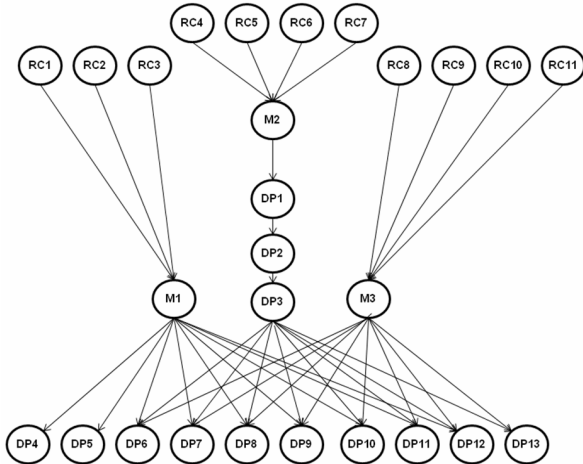


Fig. 6. Bayesian network for the implementation.

Table 5. Nodes description for Network of Fig. 6

Node	Description	Node	Description
RC1	Power loss in coaxial cable	DP1	Source forward reading
RC2	Coaxial cable loose connection	DP2	Bias forward reading
RC3	Matcher fault	DP3	RF Matcher: Current 1
RC4	MFC miscalibration	DP4	RF Matcher: Current 2
RC5	Gas line leakage	DP5	RF Matcher: Bias shunt
RC6	Gas cylinder empty	DP6	RF Probe: Voltage
RC7	Gas control valve failure	DP7	RF Probe: Current
RC8	Chamber wall deposition	DP8	RF Probe: Phase
RC9	Particles	DP9	RF Probe: DC bias
RC10	Chamber leak	DP10	TGV Current Position
RC11	Gasket/O-ring wear out	DP11	Gas12 Flow
M1	RF Module	DP12	Splitter flow total
M2	Gas Delivery Module	DP13	Splitter flow 1
M3	Process Chamber Module		

Table 6. Prior probabilities assigned to root nodes

Node	P (True)	P (False)
RC1	0.30	0.70
RC2	0.10	0.90
RC3	0.20	0.80
RC4	0.40	0.60
RC5	0.30	0.70
RC6	0.10	0.90
RC7	0.20	0.80
RC8	0.20	0.80
RC9	0.30	0.70
RC10	0.35	0.65
RC11	0.10	0.90

were performed in GeNIe [10-12]. Next, the prior probabilities and conditional probabilities were added to the network. The prior probabilities of the root nodes, RC1-RC11 are determined using historical information

Table 7. CPDS Assigned to Module Nodes

Condition			Probability	
RC1= True	RC2= True	RC3= True	P (M1= True)=0.90	P (M1= False)=0.10
RC1= True	RC2= True	RC3= False	P (M1= True)=0.85	P (M1= False)=0.15
RC1= True	RC2= False	RC3= True	P (M1= True)=0.80	P (M1= False)=0.20
RC1= True	RC2= False	RC3= False	P (M1= True)=0.85	P (M1= False)=0.15
RC1= False	RC2= True	RC3= True	P (M1= True)=0.75	P (M1= False)=0.25
RC1= False	RC2= True	RC3= False	P (M1= True)=0.70	P (M1= False)=0.30
RC1= False	RC2= False	RC3= True	P (M1= True)=0.40	P (M1= False)=0.60
RC1= False	RC2= False	RC3= False	P (M1= True)=0.10	P (M1= False)=0.90

Table 8. CPDS Assigned to Data Parameter Nodes

Condition	Probability	
M2= True	P (DP1= True)=0.85	P (DP1= False)=0.15
M2= False	P (DP1= True)=0.15	P (DP1= False)=0.85

and expert knowledge as shown in Table 6.

Similarly, utilizing process and equipment information as well as expert knowledge we assign the conditional probabilities for the module nodes M1, M2 and M3 and for data parameter nodes DP1-DP13. The values for M1 and DP1 are given as example in Tables 7 and 8 respectively. This is a critical step and the performance of the diagnostic system depends on this information.

Next step is adding the evidence for fault to the network. In order to generate fault evidence for the five faulty runs, Elman’s recurrent neural network (ERNN) models were employed, which consist of two-layer back propagation network with feedback connections from the hidden nodes to additional nodes, called the “context units” which contain the previous states of the hidden nodes [13]. The healthy runs were used for training the network for which the Levenberg Marquardt (LM) back-propagation algorithm was used due to its better performance on time series data [14]. The number of hidden neurons was varied and the network for trained for fixed number of epochs to find the structure that gave the least amount training error as shown in Table 9.

Once the network was trained for the prediction of one step ahead, it was applied on the faulty runs. The predicted and the actual observations were compared to find the root-mean-squared-error (RMSE). The normalized modeling results for the runs being diagnosed are summarized in Table 10. From the results of ERNN, we fixed a threshold of 0.45 to be the value above which an evidence of fault is considered to have been found. Values below this threshold are not considered as

Table 9. ERNN Architecture selected for each Parameter

Par.	NN Architecture	Par.	NN Architecture
1	(1-12-1)	9	(1-6-1)
2	(1-10-1)	10	(1-12-1)
3	(1-10-1)	11	(1-8-1)
4	(1-10-1)	12	(1-4-1)
5	(1-8-1)	13	(1-12-1)
6	(1-6-1)	14	(1-6-1)
7	(1-12-1)	15	(1-8-1)
8	(1-12-1)		

Table 10. ERNN results used for evidence in Bayesian Network

	Exp.1	Exp.2	Exp.3	Exp.4	Exp.5
Par.1	0.557	1	0.268	0.412	0.652
Par.2	0.756	0.385	0.245	0.976	0.863
Par.3	0.493	1	0	0.352	0.859
Par.4	0.179	0.441	0.459	0.765	1
Par.5	0.515	0.577	0.634	0	0.446
Par.6	0.413	0.309	0	0.771	1
Par.7	0.125	0.071	0.62	0.452	1
Par.8	0	0.092	0.016	0.624	1
Par.9	0.709	0.422	0.665	0.061	1
Par.10	0.697	1	0.222	0.97	0.867
Par.11	0.492	1	0.447	0.467	0
Par.12	0.337	0	1	0.196	0.926
Par.13	0.462	0.04	0.603	0	0.194
Par.14	0.002	0.003	1	0.017	0.002
Par.15	0.285	0.515	0.306	0.748	0.88

significant evidence. The value of the threshold can be modified by engineering insight in application. Then these results were incorporated in the network as evidence of fault for each run. For example for Run 20, the evidence of fault is found for the data parameters Par 1, 2, 3, 5, 9, 10, 11 and 13 (because they have value greater than fixed threshold of 0.45).

After inserting these evidences to their corresponding nodes in the network, the beliefs are updated for all other

nodes in the network. This involves performing inference (as explained in previous section) using the newly added evidences, at all nodes, stepwise going up till all beliefs are updated. The clustering algorithm was used for inference, which is the fastest exact inference algorithm [15]. At this point the root cause nodes at the top layer give the result of diagnostic inference. The node with highest value of belief among the root cause nodes would be the most probable root cause of the fault in a run. The inference results are represented in Table 11 where the maximum value of the belief for each run is highlighted. For example for Exp.1 the maximum probability is 0.57 corresponding to MFC miscalibration, so according to this diagnosis result, the MFC miscalibration is found to be the most probable root cause for this run. This diagnosis is correct because Exp.1 was induced with the same fault. Similarly Exp.2, Exp.4 and Exp.5 are also diagnosed correctly. Exp.2 however, is diagnosed to have the MFC miscalibration as the root cause of fault which was actually induced with abnormal power delivered through bias RF cable. Four out of five faults were correctly diagnosed by the system, which shows that the proposed framework can be very effective to find out the root cause of faults that occur in semiconductor etch equipment.

V. CONCLUSION

A framework to model and diagnose the semiconductor equipment using BN has been presented by incorporating the historical information and expert knowledge to design the network's structure and behavior. It was shown that by dividing the equipment into subsystems, the cause and effect relationships between different modules can be effectively modeled which then

Table 11. Inference results for Diagnosis of faults

	Power loss in Coaxial Cable	Coaxial Cable Loose Connection	Matcher Problem	MFC Mis-Calibration	Gas Line Leakage	Gas Cylinder Empty	Gas Control Valve Failure	Chamber Wall Deposition	Particles	Chamber Leak	Gasket or O-ring Leakage
Exp.1	0.47	0.15	0.24	0.57	0.36	0.14	0.23	0.22	0.33	0.46	0.12
Exp.2	0.37	0.12	0.22	0.44	0.31	0.11	0.21	0.22	0.32	0.43	0.11
Exp.3	0.39	0.13	0.22	0.57	0.36	0.14	0.23	0.21	0.32	0.36	0.11
Exp.4	0.48	0.15	0.24	0.44	0.31	0.11	0.21	0.22	0.34	0.47	0.12
Exp.5	0.53	0.16	0.25	0.50	0.34	0.12	0.22	0.24	0.36	0.56	0.13

makes the fault diagnosis a more rational process. Utilizing this technique would result in faster and more accurate diagnosis which would then considerably increase the manufacturing yield. It can be concluded that Bayesian network can be very effective tool for diagnosing faults in semiconductor etch equipment. With Bayesian network based diagnosis systems being widely benefiting in other fields, active research in this area may one day lead to an accurate automated equipment diagnosis system that could revolutionize the traditional way of manually diagnosing faults in the semiconductor industry.

ACKNOWLEDGMENTS

This work was supported by 2014 Myongji University research fund and authors are very grateful to SPDRC members for the numerous support and discussion.

REFERENCES

- [1] S. J. Hong, et al, "Fault Detection and Classification in Plasma Etch Equipment for Semiconductor Manufacturing e-Diagnostics," *IEEE Trans. Semi. Manufac.*, Vol.16, No.1, pp.83–93, Feb., 2012.
- [2] B. E. Goodlin, et al, "Simultaneous Fault Detection and Classification for Semiconductor Manufacturing Tools," *J. Electrochem. Soc.*, Vol. 150, No.12, pp. G778-G784, Dec., 2003.
- [3] A. M. Ison and C. J. Spanos, "Fault Diagnosis of Plasma Etch Equipment," *In Proc. Int. Symp. Semi. Manufac.*, San Francisco, CA, pp.B49-B52, Oct., 1997.
- [4] L. J. Barrios and L. Lemus, "Autoassociative Neural Networks for Fault Diagnosis in Semiconductor Manufacturing," *In Proc. 11th Int. Conf. on Ind. Eng. App. of Artificial Intelligence and Expert Systems*, Castellón, Spain, pp.582-592, Jun., 1998.
- [5] S. Baluja and R. A. Maxion, "Artificial Neural Network Based Detection and Diagnosis of Plasma-Etch Faults," *J. Intel. Sys.*, Vol 7, No.1-2, pp.57–82, May., 2011.
- [6] J. Pearl, "Fusion, propagation, and structuring in belief networks," *Artificial Intelligence*, Vol.29, No.3, pp.241–288, Sep., 1986.
- [7] G. S. May and C. J. Spanos, *Fundamentals of Semiconductor Manufacturing and Process Control*, New York, NY: John Wiley and Sons, 2005.
- [8] K. Pearson, "Principal Components Analysis," *The London, Edinburgh and Dublin Philosophical Magazine and Journal*, Vol.6, No.2, pp.559, 1901.
- [9] E. J. Keogh and M. J. Pazzani, "Derivative dynamic time warping," *In First SIAM Int. Conf. on Data Mining*, Chicago, USA, Apr., 2001.
- [10] GeNIe & SMILE, <http://genie.sis.pitt.edu/>.
- [11] P. A. Aguilera, et al, "Bayesian Networks in Environmental Modeling," *Env. Modeling & Software*, Vol.26, No.12, pp. 1376-1388, Dec., 2011.
- [12] S. Salini and R. S. Kenett, "Bayesian Networks of Customer Satisfaction Survey," *J. App. Statistics*, Vol.36, No.11, pp.1177-1189, Oct., 2009.
- [13] J. L. Elman, "Finding Structure in Time," *Cognitive Science*, vol. 14, no. 2, pp. 179-211, Apr., 1990.
- [14] E. K. Levenberg, "A Method for the Solution of Certain Non-Linear Problems in Least Squares," *The Quart. App. Math.*, vol. 2, pp. 164-168, Jul., 1944.
- [15] S. S. Lauritzen and D. J. Spiegelhalter, "Local computations with probabilities on graphical structures and their application to expert systems", *J. the Royal Statistical Society*, Vol.B 50, No.2, pp.253-258, 1988.



Javeria Muhammad Nawaz received her BS degree in Electronics Engineering from Bahria University, Pakistan in 2009 and MS degree in Electronics Engineering from Myongji University, Korea in 2013. Her research interest is semiconductor process data mining using various statistical analysis techniques.



Muhammad Zeeshan Arshad received the BS degree in Electronics Engineering from Bahria University, Pakistan in 2009 and MS degree in Electronics Engineering from Myongji University, Korea in 2013. Currently he is pursuing his doctoral degree in

the same university. Mr. Arshad is a member of the Semiconductor Process Diagnosis Research Center (SPDRC) at Myongji University. Since 2013, Mr. Zeeshan has also been working as software developer at Rainbow Corporation (RBC). His research interest is mainly software development for the purpose of real-time semiconductor process monitoring and diagnosis.



Sang Jeon Hong received his B.S. in ECE from Myongji University, Korea in 1992 and his M.S. and Ph.D. degree in ECE from Georgia Institute of Technology, Atlanta, in 2001 and 2003. His research interents are APC with *in-situ* sensors and tool data

driven FDC in volume semiconductor manufacturing. He is currently an associate professor in the Department of Electronic Engineering at Myongji Unviersity, where he serves as a director of semiconductor process diagnosis research center (SPDRC). Dr. Hong is also serving a Director of Cooperative Center for Research Facilities at Myongji University. Dr. Hong was Editor-in-Chief of Transactions on Electrical and Electronic Materials from 2006-2007, and has been listed Marquies' Who's Who in the World from 2009-2014. He held JSPS Fellowship at Tohoku University, and has worked at IBM in Eash Fishkill as a process engineer.